Glutamate induces the rapid formation of spine head protrusions in hippocampal slice cultures

David A. Richards*†, José Maria Mateos*, Sylvain Hugel*, Vincenzo de Paola‡§, Pico Caroni‡, Beat H. Gähwiler*¶, and R. Anne McKinney*‖

*Brain Research Institute, University of Zurich, Winterthurerstrasse 190, CH-8057 Zurich, Switzerland; and ‡Friedrich Miescher Institute, Novartis Research Foundation, Maulbeerstrasse 66, CH-4058 Basel, Switzerland

Communicated by Harald Reuter, University of Bern, Bern, Switzerland, March 8, 2005 (received for review October 25, 2004)

Synaptic plasticity at neuronal connections has been well characterized functionally by using electrophysiological approaches, but the structural basis for this phenomenon remains controversial. We have studied the dynamic interactions between presynaptic and postsynaptic structures labeled with FM 4-64 and a membrane-targeted GFP, respectively, in hippocampal slices. Under conditions of reduced neuronal activity (1 μM tetrodotoxin), we observed extension of glutamate receptor-dependent processes from dendritic spines of CA1 pyramidal cells to presynaptic boutons. The formation of these spine head protrusions is blocked by α-amino-3-hydroxy-5-methyl-4-isoxazole propionic acid (AMPA) receptor antagonists and by agents that reduce the release of glutamate from presynaptic terminals. Moreover, spine head protrusions form in response to exogenously applied glutamate, with clear directionality toward the glutamate electrode. Our results suggest that spontaneously released glutamate is sufficient to activate nearby spines, which can then lead to the growth of new postsynaptic processes connecting to a presynaptic site. Spines thus can compare their recent history with that of neighboring synapses and modify local connectivity accordingly.

hippocampus | pyramidal cell | FM 4-64 | GFP | Thy1

The majority of excitatory connections in the hippocampus are made at dendritic spines, which are small protrusions ($\approx$1 μm long) that extend from dendrites (1, 2). Dendritic spines can undergo significant morphological change over a timescale of seconds (3), and this motility is both actin-dependent and responsive to synaptic activity (4–7). Spine motility plays a major role in synaptogenesis (8–10) but its physiological relevance in mature spines is unknown. It has been suggested that spine motility influences the compartmentalization of electrical and calcium signals, yet in CA1 pyramidal cells the resistance of the spine neck is insufficient for electrical filtering (11), and spine dynamics will have no effect on calcium signaling because calcium diffusion through the neck is negligible (12). Recent work from our laboratory also indicates a relationship between spine motility and the ability of proteins tethered to the inner leaflet of the membrane to diffuse (13). We have further explored possible physiological roles of spine motility by investigating dynamic interactions between presynaptic and postsynaptic sites and the regulation of these dynamics by glutamate. Our results indicate that the motility of mature spines can lead to changes in synaptic connectivity. We hypothesize that when a spine has not been recently activated by glutamate released by its associated bouton, it can respond to glutamate released by a neighboring synapse. Spines thus can compare their individual recent history to the level of activity of neighboring synapses and modify hippocampal microcircuitry accordingly.

Methods

Transgenic Mice. Variegated mice were generated by using standard techniques. A construct was generated where the cDNA for EGFP was fused to the membrane-anchoring domain (first 41 aa) of a palmitoylated mutant of MARCKS29, under the Thy1 promoter. Twenty-five distinct lines were generated, each with subtly different patterns of expression (14). Of these, L15 mice were chosen because they had low but consistent levels of membrane-targeted GFP (mGFP)-positive cells within area CA1 of the hippocampus.

Slice Cultures. Organotypic slice cultures were used for these experiments because they provide the major advantage of exhibiting preserved tissue-specific organization of synaptic connections, in an *in vitro* preparation suitable for imaging studies. Slices (400 μm) were prepared from the hippocampi of 6-day-old L15 mice and maintained in roller tubes for 3–6 weeks before use, as described for rat in ref. 15.

Confocal Imaging. Slice cultures were transferred to a recording chamber mounted on an upright microscope (DMLFSA, Leica Microsystems, Heidelberg) equipped with a heated (30°C) submersion chamber where slices were continually perfused with a solution comprising 137 mM NaCl, 2.7 mM KCl, 2.5 mM $CaCl_2$, 2 mM MgCl, 11.6 mM $NaHCO_3$, 0.4 mM NaH_2PO_4, and 5.6 mM glucose. The confocal scanhead was a Leica SP2. EGFP was imaged by using the 488-nm laser line, with voxel dimensions of $46 \times 46 \times 200$–250 nm. Tertiary and some secondary dendrites of the EGFP-labeled pyramidal cells were imaged by using a $\times$63 water immersion long working distance lens. Additional optical sections were taken above and below the structure of interest to allow for any changes in the structure with time. Once the images were captured, the area of interest was cropped and further processed. FM 4-64 (10 μM) was loaded and imaged as described in ref. 16 for FM 1-43 with the substitution of a 543-nm laser line for excitation. FM 4-64 was applied in two ways: to label either the majority of terminals in a preparation or only a few boutons. To label the majority of terminals, FM 4-64 was applied via a patch pipette in the stratum radiatum in the presence of bicuculline (50 μM), and afferent fibers were then stimulated with an electrode placed in area CA1 (10 Hz, 5 min). FM 4–64 and bicuculline were subsequently washed out with a Tyrode solution containing 1 mM Advasep-7 and 0.5 μM tetrodotoxin (TTX), and then the slice was imaged. To label just a few boutons, the stimulation intensity and duration were reduced (90 s at 10 Hz or 20 s at 40 Hz), and no bicuculline was used. FM 4-64 was again washed out by using Advasep-7 and TTX.

Freely available online through the PNAS open access option.

Abbreviations: AMPA, α-amino-3-hydroxy-5-methyl-4-isoxazole propionic acid; mGFP, membrane-targeted GFP; NBQX, 1,2,3,4-tetrahydro-6-nitro-2,3-dioxo-benzo[*f*]quinoxaline-7-sulphonamide; SHP, spine head protrusion; TTX, tetrodotoxin.

†Present address: Department of Cell Biology, Neurobiology, and Anatomy, Vontz Center for Molecular Studies, 3125 Eden Avenue, Cincinnati, OH 45267-0521.

§Present address: Cold Spring Harbor Laboratory, 1 Bungtown Road, Cold Spring Harbor, NY 11724.

¶To whom correspondence should be addressed. E-mail: gahwiler@hifo.unizh.ch.

‖Present address: Department of Pharmacology and Therapeutics, McGill University, 3655 Promenade Sir-William-Osler, Montréal, QC, Canada H3G 1Y6.

www.pnas.org/cgi/doi/10.1073/pnas.0501881102

Electron Microscopy. After TTX treatment (2 h), hippocampal slice cultures were fixed with 2.5% glutaraldehyde and 1% paraformaldehyde in 0.1 M phosphate buffer (pH 7.4), osmicated, and embedded in Epon resin. CA1 stratum radiatum region was trimmed, and ultrathin serial sections were collected. Ultramicrographs were taken at a magnification of ×20,000 with a digital camera (Gatan 791 multiscan, Pleasanton, CA) attached to a Zeiss EM 10 electron microscope.

3D Reconstruction. Image stacks (4D) were deconvolved by using HUYGENS PRO software (Scientific Volume Imaging, Hilversum, The Netherlands, supplied by Bitplane, Zurich) running on a Silicon Graphics Octane workstation (Mountain View, CA), by using a full maximum likelihood extrapolation algorithm. Volume rendering and quantification was carried out by using IMARIS SURPASS software (Bitplane) running on a WINDOWS 2000 workstation (Professional version, Microsoft). The same parameters were used for all time points of an experimental series.

Iontophoresis. Patch electrodes (10 MΩ) were filled with 1 mM glutamate. Iontophoretic and holding currents were applied by a microiontophoresis programmer (WPI Instruments, Sarasota, FL). Trigger pulses were generated by a Master-8 programmable pulse generator (A.M.P.I., Jerusalem). Current alone (i.e., no glutamate) and glutamate together with 1,2,3,4-tetrahydro-6-nitro-2,3-dioxo-benzo[*f*]quinoxaline-7-sulphonamide (NBQX; 10 μM) did not elicit spine head protrusions (SPHs) (n = 4 slices for each paradigm).

Reagents. CPP was donated from Novartis (Basel); TTX was obtained from Latoxan (Valence, France), FM 4-64 was obtained from Molecular Probes Europe (Leiden, The Netherlands), and Advasep-7 was obtained from CyDex (Overland Park, KS); all other reagents were from either Tocris Cookson (Bristol, U.K.) or Sigma.

Results

Dendritic spines were visualized by transgenic expression of mGFP in a subset of neurons in mouse slice cultures (14), allowing for a detailed analysis of axonal and dendritic outlines of individual living pyramidal cells. Labeled cells had characteristic pyramidal cell morphology (Fig. 1*A*), and mGFP fluorescence extended throughout dendritic spines (Fig. 1*B*). Spine lengths and interspine distances were similar to those reported previously for rat slice cultures (mean spine length, 1.09 ± 0.08 μm; mean interspine distance, 1.02 ± 0.04 μm; n = 328 spines from 21 cells in 21 slices; compare with ref. 15). This combination of restricted mGFP expression with advanced reconstruction techniques has enabled us to monitor the full 3D structure of dendritic spines over time.

SHPs During Application of TTX. Increasing evidence suggests that inactivity extending for days induces changes in the structure and function of hippocampal synapses, although the characteristics of these reported changes differ (15, 17, 18). Long-term exposure of neurons to TTX led to increases in spine density in the lateral geniculate nucleus (17) and in the number of dendritic filopodia on CA1 pyramidal cells (15). We have investigated the acute effects of reduced activity on dendritic spines. Perfusion of hippocampal slices with TTX (1 μM) led to the formation within an hour of intriguing structures consisting of fine filopodia-like processes emanating from the spine head and exhibiting a terminal swelling (Fig. 1 *C* and *D*). These SHPs also could be seen to form during time-lapse experiments (Fig. 1*C*; see also Movie 1, which is published as supporting information on the PNAS web site). We did not include filopodia extensions originating from dendrites in our analysis. On average 0.96 ± 0.17 SHPs were detectable per 10 μm of dendrite after 60-min exposure to TTX (163 μm of tertiary apical dendrites examined from five slices; see also Fig. 2*A*). The protrusions were seen to extend smoothly in an undeviating fashion, as though they were responding to an external guidance cue.

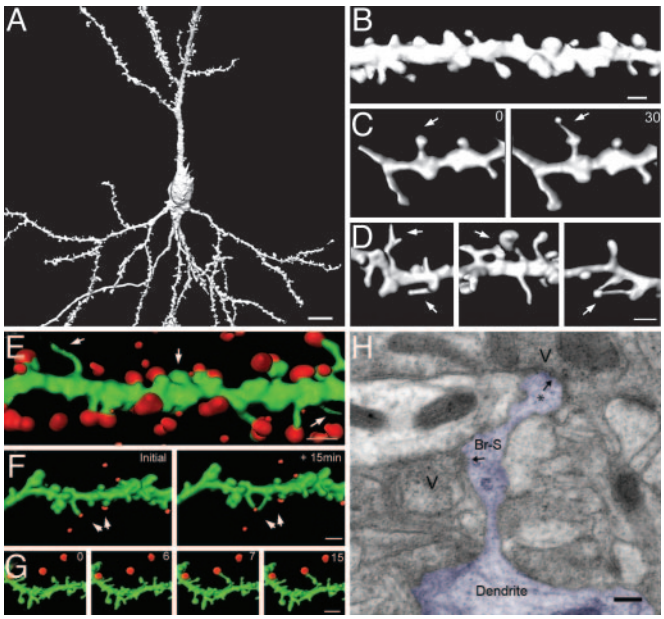

Fig. 1. The formation of SHPs. (*A*) A 3D reconstruction of a typical CA1 pyramidal neuron expressing mGFP. (Scale bar: 10 μm.) (*B*) Example of a stretch of tertiary apical dendrite at higher magnification. (Scale bar: 1 μm.) (*C*) TTX induces the formation of SHPs. A short stretch of dendrite is shown immediately before (*Left*) and 30 min after (*Right*) the application of 1 μM TTX. Arrow indicates the location of a spine that converts into a SHP. (*D*) More examples of SHPs formed during TTX treatment. Arrows indicate the location of a spine that converts into a SHP. (Scale bar: 1 μm.) (*E*) Maximal labeling of functional boutons with FM 4-64 reveals that the majority of dendritic spines are apposed to FM 4-64 puncta. Arrows indicate one spine without label (center) and two filopodia also without label. (Scale bar: 1 μm.) (*F*) Example of a stretch of dendrite double-labeled with mGFP (green) and FM 4-64 (red) at the beginning (*Left*) and end (*Right*) of a 15-min experiment. Arrows mark the formation of a SHP. (*G*) A separate experiment showing a subfield (time elapsed during image series is given in minutes in the top right corner). (*H*) Electron micrograph of a SHP (Br-S, branched spine) with a process (*) emerging from the spine head, displaying a postsynaptic density. The initial spine (Br-S) with a putative postsynaptic density is opposed to a presynaptic bouton. Vesicle clusters are illustrated (V) for both apparent synaptic contacts, which are indicated by arrows. (Scale bar: 0.2 μm.)

Labeling of Presynaptic and Postsynaptic Sites. Although action potential-evoked release is blocked by TTX, spontaneous vesicular release still occurs. Therefore, the SHPs may be a response to glutamate released from nearby presynaptic terminals. To address this possibility, we visualized presynaptic elements adjacent to the dendrites of interest by focally applying the styryl dye FM 4-64 from a pipette placed in stratum radiatum, coupled with electrical stimulation (10 Hz for 5 min) in the presence of bicuculline (50 μM) to maximize the number of boutons activated. The resultant staining was punctate and could be destained by subsequent stimulation (data not shown), consistent with labeling of synaptic vesicles. Sections of mGFP-labeled dendrite adjacent to FM 4-64 puncta were then imaged. The resulting FM 4-64 labeling was dense (0.55 ± 0.16 boutons per μm^3; n = 4,312 boutons from four slices), labeling presynaptic structures apposed to the majority of dendritic spines (Fig. 1*E*; 78 of 89 spines examined had a bouton closely apposed). These data provide evidence that most, if not all, dendritic spines are

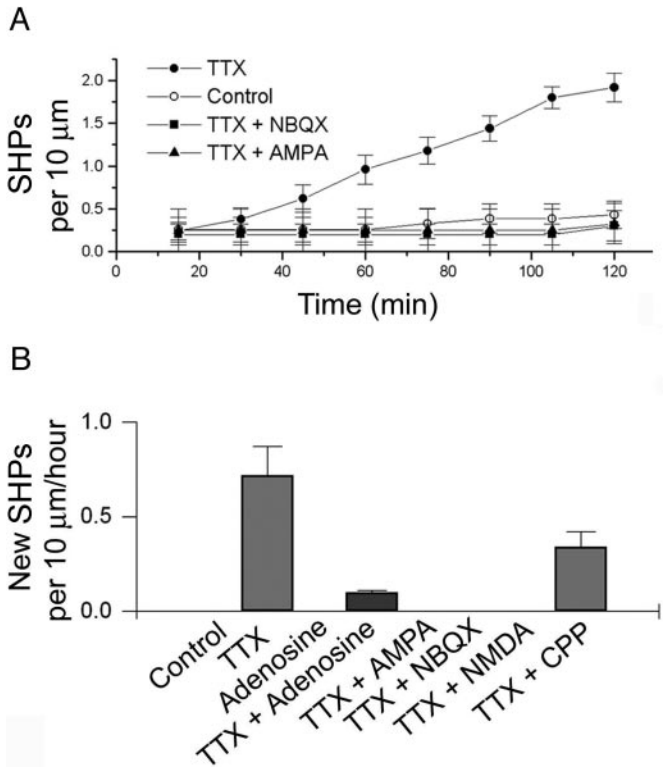

Fig. 2. The formation of SHPs depends on glutamate receptor activation and presynaptic release. (*A*) The emergence of SHPs as a function of time in TTX. The effect of TTX was blocked by coapplication with either AMPA (0.5 μM) or NBQX (10 μM). (*B*) Quantification of the appearance of new SHPs per hour per 10 μm of dendrite during application of adenosine (50 μM), AMPA (0.5 μM), NMDA (1 μM), the AMPA receptor antagonist NBQX (10 μM), and the NMDA receptor antagonist CPP (50 μM). Data are from four to six slices per point.

in contact with presynaptic boutons, but such a strong stimulus is likely to cause presynaptic and postsynaptic changes (the latter are perhaps indicated by the slightly swollen appearance of the dendritic shaft in Fig. 1*E*). We therefore carried out experiments to investigate whether the SHPs contacted presynaptic elements by using a much more modest labeling strategy. By coupling dye application with weak stimulation (90 s at 10 Hz or 20 s at 40 Hz), we were able to label only a few axons, which we could then see as tracks of puncta traversing the slice. This milder stimulation used for loading the FM dye had no significant effect on spine morphology (spine volume before, 0.34 $\pm$ 0.11 μm^3; and after gentle FM loading, 0.3 $\pm$ 0.17 μm^3; $n = 68$ spines from six slices; paired t test, $P > 0.05$). By combining this labeling approach with time-lapse imaging of regions where labeled axons and dendrites came into close proximity with one another, we were able to observe protrusions extending toward glutamate release sites, as though they were responding to an external cue (Fig. 1 *F* and *G* and Movie 1).

Although the FM 4-64 experiments demonstrate SHPs terminating at functional presynaptic boutons, this observation by itself does not provide evidence that functional synapses are formed. To address this point, we examined the ultrastructure of SHPs formed during a 2-h incubation with TTX. Fig. 1*H* shows an electron micrograph of such a SHP. The micrograph not only illustrates that the original spine head possesses a postsynaptic density aligned with a presynaptic bouton with an active zone but also reveals another synaptic contact at the end of the process. This new synaptic contact also possesses both a postsynaptic density and an apparent release site. This finding suggests that the formation of SHPs does indeed correspond to a change in synaptic connectivity (see also *Supporting Data*, which is published as supporting information on the PNAS web site).

Pharmacological Profile of the Formation of SHPs. The time-dependent formation of SHPs (Fig. 1*C*) provided us with a means of characterizing the pharmacological profile for the formation of these processes (after 2 h, control slices showed 0.23 $\pm$ 0.24 SHPs per 10 μm of dendrite, compared with 1.94 $\pm$ 0.16 in TTX, in five slices). Because *N*-methyl-D-aspartate (NMDA) receptors are blocked by Mg^{2+} ions at resting membrane potentials, we chose to investigate the involvement of α-amino-3-hydroxy-5-methyl-4-isoxazole propionic acid (AMPA) receptors in the formation of SHPs. Inclusion of the AMPA receptor antagonist NBQX (10 μM) in the medium prevented the TTX-dependent appearance of SHPs (Fig. 2*A*), indicating a requirement for AMPA receptor activation. AMPA receptor activation has also been shown to have a strong inhibitory effect on spine motility in hippocampal neurons *in vitro* (*5*); we therefore determined whether the addition of AMPA would enhance or prevent the formation of SHPs. Imaging regions of dendrite in the presence of both AMPA (0.5 μM) and TTX, we found that AMPA prevented the appearance of SHPs (Fig. 2; no new SHPs were seen to form over 1 h in $\approx$60 μm of dendrite from five slices, compared with 0.72 $\pm$ 0.15 in TTX alone), consistent with the stabilizing effect of AMPA on dendritic spines. Thus, AMPA activates spines and in effect "drowns out" the signal from the presumed spillover glutamate, whereas NBQX renders spines insensitive to glutamate. We extended this approach to other pharmacological treatments, as summarized in Fig. 2*B*. Importantly, we found that 50 μM adenosine, which causes a pronounced (>80%) presynaptic depression in this preparation (19), almost completely abolished the appearance of these TTX-induced structures (0.11 $\pm$ 0.01 per 10 μm of new SHPs formed over the course of 1 h; $\approx$75 μm of dendrite from six slices) indicating that spontaneous vesicular release of glutamate is sufficient to trigger the induction of SHPs. Furthermore, other experiments indicate a possible role for NMDA receptors in this process. Application of NMDA itself (1 μM), in low Mg^{2+} solution, prevented the appearance of new SHPs, and application of 50 μM CPP (a competitive NMDA receptor antagonist) also reduced the effect of TTX (0.34 $\pm$ 0.08 new SHPs formed per 10 μm of dendrite). Because NMDA receptors have been shown to be activated by single quanta of glutamate in an AMPA receptor-dependent manner (20), this result suggests that activation of both NMDA and AMPA receptors is necessary.

Effects of Exogenously Applied Glutamate. If synaptic release of glutamate initiates the formation of SHPs, we reasoned that SHPs might form after a brief focal pulse of exogenously applied glutamate. We therefore perfused slices with TTX and placed an iontophoresis electrode containing 1 mM glutamate $\approx$10 μm from the dendrites to be imaged. Low currents ($\leq$100 nA iontophoresis currents) caused outgrowth of SHPs (see Fig. 3 *A–E*). The proportion of spines forming protrusions within 8 min after a glutamate pulse was far greater than would be expected in preparations treated with TTX alone (1.95 $\pm$ 0.18 per 10 μm from 110 μm of imaged dendrite from seven slices, compared with <0.1 per 10 μm over a similar time in TTX-treated preparations; see Fig. 3*F*; $P < 0.001$). Iontophoretically applied glutamate did not induce toxic effects, because spine volume did not significantly change after glutamate pulses (0.32 $\pm$ 0.11 μm^3 to 0.30 $\pm$ 0.15 μm^3; $n = 74$ spines; from six slices; paired t test, $P > 0.05$). Not all spines responded, however, to iontophoretically applied glutamate, which may reflect heterogeneity of spine sensitivity or differences in diffusional access due to intervening glial and neuronal processes. As shown in the pooled data in Fig.

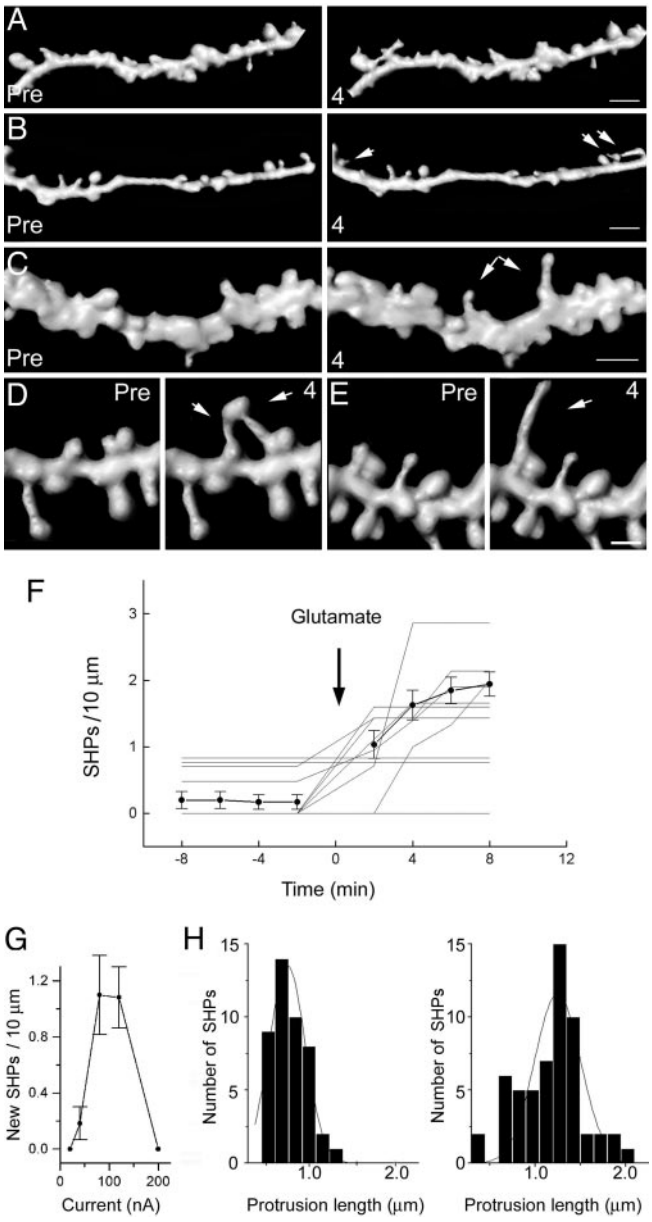

Fig. 3. Focal glutamate pulses induce the formation of SHPs. (*A–C*) Stretches of dendrite viewed before (0 min; *Left*) and after (4 min; *Right*) iontophoretically applied glutamate pulses during TTX treatment. Arrows indicate newly formed SHPs. (Scale bar: 2 μm.) (*D* and *E*) Two additional experiments with an area of interest shown at higher magnification. (Scale bar: 1 μm.) (*F*) Time dependence of the response to iontophoretically applied glutamate. The mean number of SHPs $\pm$ SEM is plotted against time. A pulse of glutamate was applied as indicated. Individual data are also plotted as thin lines. Sections of dendrite that did not respond to glutamate were excluded from the mean value shown. (*G*) Bell-shaped dependence of the formation of SHPs on the iontophoresis current. Low ejection currents elicited no SHP formation. Increasing current elicited SHPs and then failed at the highest ejection currents. (*H*) Spontaneously occurring SHPs form shorter processes than those that respond to glutamate application. The length of processes extending from the heads of SHPs are plotted to show their distribution. (*Left*) Processes that occurred spontaneously during TTX treatment. (*Right*) Processes that formed in response to iontophoretic application of glutamate.

3*F*, those spines that did respond to glutamate did so within 8 min of agonist application. The delay in the formation of SHPs is unlikely to be due to diffusion but rather may reflect biochemical processes within the spine, which mediate this response to glutamate.

The iontophoretic approach enabled us to semiquantitatively address the dependence of the formation of SHPs on glutamate concentration. Fig. 3*G* shows an initial increase in the number of SHPs formed proportional to the amplitude of the iontophoretic current, followed by a subsequent decrease as the current increases further. This result supports our previous finding that application of AMPA or NMDA prevents the formation of SHPs by drowning out other signals. As summarized in Fig. 3*H*, iontophoretically induced SHPs had a longer mean length than those that occurred spontaneously in TTX, suggesting that under the latter conditions, SHPs spontaneously extend until they reach a valid target (presynaptic bouton).

Because SHPs occurred in response to glutamate, they might show some kind of directionality. We therefore measured the angle between spine head and iontophoresis electrode and compared it with the angle taken by SHPs (Fig. 4*A*). Although SHPs that formed spontaneously (before the glutamate pulse) were randomly distributed, those that followed the glutamate pulse were all closely aligned with the electrode, indicating that they do indeed form with directionality imparted by the eliciting stimulus.

To investigate how SHPs are related to previously described forms of spine motility, we first investigated the impact of iontophoretic application of glutamate on spine motility (Fig. 4*B*). Consistent with previous reports where AMPA was bath-applied (5), we found that glutamate induced an abrupt drop in motility (measured as fluctuation in apparent spine volume), which then recovered with a $t_{1/2}$ of 17 min. We also found that application of relatively strong ejection currents (200 nA) caused spines to become refractory for the generation of new SHPs (Fig. 4*C*), as though the spines possessed some sort of biochemical memory of their recent ($\approx$20 min) history. A further area of investigation was the stability of SHPs. As Fig. 4*D* shows, application of a "weak" pulse of glutamate (80 nA) led to the appearance of SHPs as described above. We then applied a second pulse of glutamate at time Δt (from 2 to 20 min). This second, stronger glutamate pulse (200 nA) applied immediately after the first caused SHPs to retract. Interestingly, they gained stability over time, so that pulses applied 20 min after the initial pulse had elicited the formation of SHPs had no effect. This result suggests that SHPs rapidly mature over the first 10 min or so after their formation.

Discussion

In the present work, we provide evidence linking the extrusion of processes from the spine head to the presence of glutamate. The formation of SHPs is blocked by NBQX (which prevents spines from sensing glutamate via AMPA receptors) and also by AMPA (which stabilizes spines). These processes "reach out" to contact nearby boutons and appear to form new synapses. Our hypothesis is further strengthened by the observation that exogenously applied glutamate triggers the formation of protrusions. We have imaged SHPs for up to 3 h and found the SHPs still remained (data from five separate slices). Further investigation will determine whether these SHPs are forerunners to previous observations of boutons splitting (21) and new spines emerging (22, 23).

The extent of synaptic activation can be estimated by considering typical values for the frequency of spontaneous miniature excitatory postsynaptic currents measured at the soma (1.5 Hz) compared with the estimated number of excitatory synapses on a pyramidal cell in this preparation (n = 5,000). These values would indicate that a detectable miniature event occurs on average once every hour, per synapse. Thus, even if the true frequency of spontaneous miniature events were twice this value, one would expect that a spine would only detect glutamate from its synaptic partner approximately every 30 min. Spines therefore will receive very heterogeneous patterns of activation (some will be exposed to synaptic glutamate, and some will not). If relative levels of activation, rather than absolute levels, are considered, then this mechanism can be

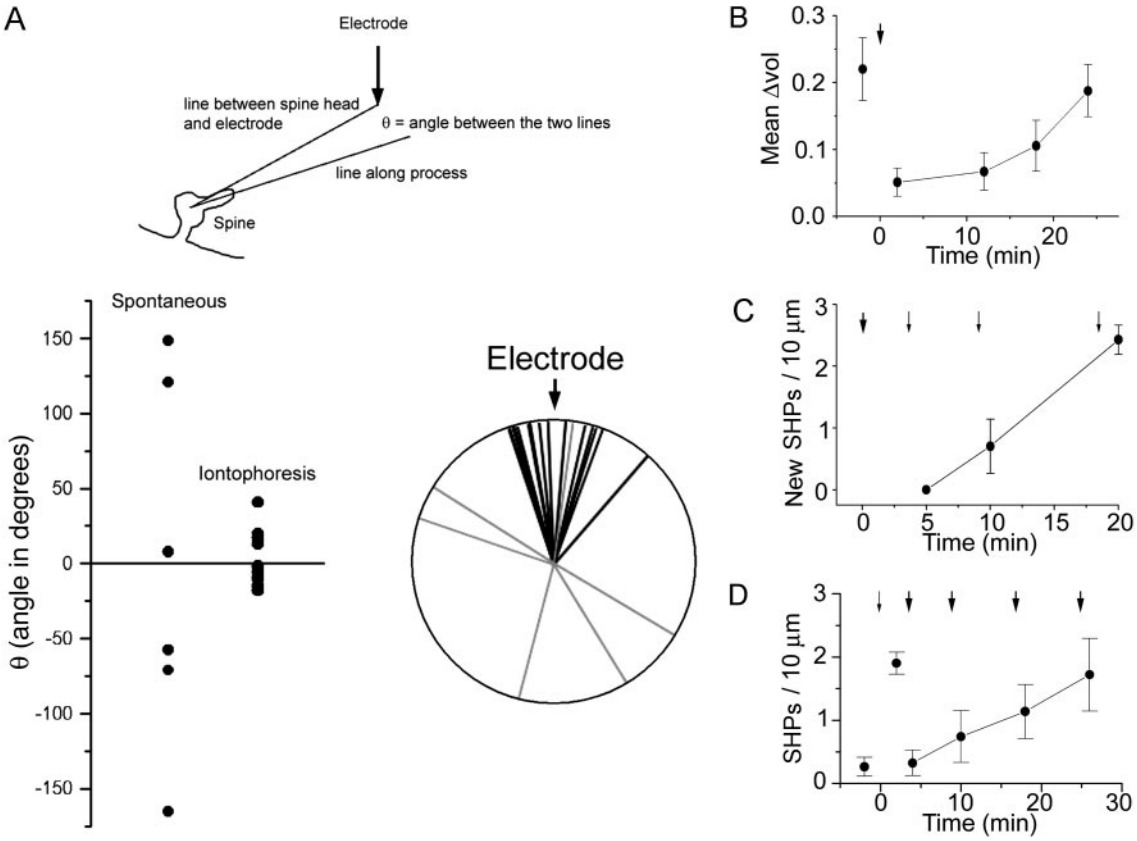

Fig. 4. Additional properties of SHPs. (*A*) Schematic diagram indicating how the angle taken by a SHP was measured. A line was drawn from the center of the spine head to the position of the iontophoresis electrode. A second line was then drawn along the SHP, from the center of the spine head. The difference represents the angle Θ. (*Lower*) Data are plotted as scatter plots (*Left*) and radial plots (*Right*). Processes that formed in the absence of iontophoretic application of glutamate (light gray in the radial plot) show no directional tendency, whereas those that formed in response to glutamate (black in the radial plot) tended to point toward the iontophoresis electrode. This figure is a summary of 12 experiments. (*B*) Spine motility takes ≈20 min to recover after iontophoretic application of glutamate. Spine motility was measured as the fluctuation in individual spine volume from a mean value. A 200-nA glutamate pulse was applied as indicated by the arrow. (*C*) The formation of SHPs becomes refractory for 10–20 min after a strong glutamate pulse. A 200-nA pulse was applied at the time indicated by the bold arrow. A weaker pulse (100 nA) then was applied after a delay of 5, 10, or 20 min. (*D*) Progressive stabilization of SHPs. After a 100-nA glutamate pulse (small arrow), SHPs appear. Subsequent challenge with a 200-nA glutamate pulse (bold arrow) at 4, 10, 18, or 26 min after the weaker pulse reveals that SHPs can be destabilized but become progressively resistant to strong glutamate pulses over time. Data in all panels are from four to six slices per point.

extended to more normal conditions. If action potentials are not blocked by TTX, two additional factors come to bear: evoked synaptic release and back-propagating action potentials. It is conceivable that the combination of back-propagating action potentials (which signal how active the postsynaptic cell is as a whole) and glutamate spillover (signaling how active nearby synapses are) enables a spine to compare its direct activation with both local (spillover) and overall (action potential) levels of activation.

Is there any evidence that such a mechanism may operate during elevated levels of activity? If a subset of inputs is much more strongly activated than their neighbors, a situation that occurs during the induction of long-lasting synaptic changes (24), a similar phenomenon (glutamate-triggered formation of SHPs) may occur. A recent ultrastructural study indicated that high-frequency stimulation of the perforant path-dentate gyrus synapse *in vivo* can give rise to SHPs (25), providing support for this hypothesis. Interestingly, new spines have been seen to emerge from dendritic shafts after tetanic stimulation (22, 23). Additionally, our observation of multiple spines contacting the same bouton (multiple synapse boutons) is strikingly similar to the increase in such structures seen in potentiated synapses at the ultrastructural level (26, 27). Furthermore, *in vivo* experiments also have shown an increase in the number of multiple synapse boutons in trace eye blink conditioned rabbits, without an increase in the total number of synapses (28). Recent electron microscopy studies have reported the formation of spinules, which are either short vesicular or long vermiform evaginations emerging from dendrites, spine heads, and axons (29). Spinules are transitory structures and considerably smaller (in the nanometer range) than the processes we have observed, which are 1–2 μm in length.

In summary, we have carried out a detailed analysis of spine dynamics under conditions of reduced synaptic input. Our finding that spines establish new contacts with nearby boutons in a glutamate receptor-dependent fashion suggests that this reaction may occur in response to glutamate spillover. We hypothesize that when a spine has not been recently activated by glutamate released by its associated bouton, it can respond to glutamate released by a neighboring synapse. Spines thus can compare their individual history (the activity they experienced over the preceding minutes) to the level of activity of neighboring synapses. Such activity-dependent adaptation of connectivity is a significant additional level of branching for neuronal networks and a previously undescribed form of synaptic plasticity.

We thank L. Heeb and L. Rietschin for excellent technical assistance, B. Zarda for advice on the microscope, P. Schwarb for support in 3D software, A. Lüthi for discussions, and M. Scanziani and U. Gerber for detailed comments on the manuscript. This work was supported by Swiss National Science Foundation Grant 31-61518.00.

1. Harris, K. M. (1999) *Curr. Opin. Neurobiol.* **9,** 343–348.
2. Hering, H. & Sheng, M. (2001) *Nature Rev. Neurosci.* **2,** 880–888.
3. Fischer, M., Kaech, S., Knutti, D. & Matus, A. (1998) *Neuron* **20,** 847–854.
4. Lendvai, B., Stern, E. A., Chen, B. & Svoboda, K. (2000) *Nature* **404,** 876–881.
5. Fischer, M., Kaech, S., Wagner, U., Brinkhaus, H. & Matus, A. (2000) *Nature Neurosci.* **3,** 887–894.
6. Dunaevsky, A., Tashiro, A., Majewska, A., Mason, C. & Yuste, R. (1999) *Proc. Natl. Acad. Sci. USA* **96,** 13438–13443.
7. Korkotian, E. & Segal, M. (2001) *Neuron* **30,** 751–758.
8. Ziv, N. E. & Smith, S. J. (1996) *Neuron* **17,** 91–102.
9. Dailey, M. E. & Smith, S. J. (1996) *J. Neurosci.* **16,** 2983–2994.
10. Marrs, G. S., Green, S. H. & Dailey, M. E. (2001) *Nature Neurosci.* **4,** 1006–1013.
11. Svoboda, K., Tank, D. W. & Denk, W. (1996) *Science* **272,** 716–719.
12. Sabatini, B. L., Oertner, T. G. & Svoboda, K. (2002) *Neuron* **33,** 439–452.
13. Richards, D. A., De Paola V., Caroni P., Gähwiler B. H. & McKinney, R. A. (2004) *J. Physiol.* **558,** 503–512.
14. De Paola, V., Arber, S. & Caroni, P. (2003) *Nature Neurosci.* **6,** 491–500.
15. McKinney, R. A., Capogna, M., Dürr, R., Gähwiler, B. H. & Thompson, S. M. (1999) *Nature Neurosci.* **2,** 44–49.
16. Zakharenko, S. S., Zablow, L. & Siegelbaum, S. A. (2001) *Nature Neurosci.* **4,** 711–717.
17. Dalva, M. B., Ghosh, A. & Shatz, C. J. (1994) *J. Neurosci.* **14,** 3588–3602.
18. Murthy, V. N., Schikorski, T., Stevens, C. F. & Zhu, Y. (2001) *Neuron* **32,** 673–682.
19. Scanziani, M., Capogna, M., Gähwiler B. H. & Thompson, S. M. (1992) *Neuron* **9,** 919–927.
20. Emptage, N. J., Bliss, T. V. & Fine, A. (1999) *Neuron* **22,** 115–124.
21. Collicos, M. A., Collins, B. E., Sailor, M. J. & Goda, Y. (2001) *Cell* **107,** 605–616.
22. Engert, F. & Bonhoeffer, T. (1999) *Nature* **399,** 66–70.
23. Maletic-Savatic, M., Malinow, R. & Svoboda, K. (1999) *Science* **283,** 1923–1927.
24. Bliss, T. V. P. & Collingridge, G. L. (1993) *Nature* **361,** 31–39.
25. Dhanrajan, T. M., Lynch, M. A., Kelly, A., Popov, V. I., Rusakov, D. A. & Stewart, M.G. (2004) *Hippocampus* **14**, 255–264.
26. Toni, N., Buchs, P. A., Nikonenko, I., Bron, C. R. & Muller, D. (1999) *Nature* **402,** 421–425.
27. Fiala, J. C., Allwardt, B. & Harris, K. M. (2002) *Nature Neurosci.* **15,** 297–298.
28. Geinisman, Y., Berry, R. W., Disterhoft, J. F., Power, J. M. & Van der Zee, E. A. (2001) *J. Neurosci.* **21,** 5568–5573.
29. Spacek, J. & Harris, K. M. (2004) *J. Neurosci.* **24,** 4233–4241.